

Significance of *YAP1–MAML2* rearrangement and *GTF2I* mutation in the diagnosis and differential diagnosis of metaplastic thymoma

Minghao Wang^a, Hongtao Xu^b, Qiang Han^b and Liang Wang^b

^aDepartment of Neurosurgery, First Hospital of China Medical University, Shenyang, China; ^bDepartment of Pathology, First Hospital of China Medical University, Shenyang, China

ABSTRACT

Background: Metaplastic thymoma (MT) is a very uncommon thymoma type, with biphasic differentiation as one of its histological characteristics. This histological pattern, however, can also be mistaken for type A thymoma and the A component in type AB thymoma.

Methods: Postoperative specimens were collected from five MT and four type A thymomas with a retrospective analysis involving immunohistochemistry, fluorescence *in situ* hybridization (FISH) and next-generation sequencing (NGS).

Results: The histological morphology of the MT overlapped with that of the type A thymoma. With immunostains, the former's spindle cell components expressed vimentin and EMA, but not CD20. In MT, 3/5 cases had the nuclear expression of YAP1. The spindle cell component of the type A thymoma was found to express CD20. In all five cases of MT, FISH detection revealed *YAP1–MAML2* fusion, which was not found in any type A thymoma cases. NGS sequencing confirmed *YAP1–MAML2* rearrangement in all five cases of MT, and mutations in *POLE* and *HRAS* were also found in two cases, respectively. *GTF2I* c.74146970 T>A mutations were found in all cases of type A thymoma, and *HRAS* and *NRAS* mutations were found in two cases, but no *YAP1–MAML2* rearrangement was evident.

Conclusions: For the diagnosis and differential diagnosis of challenging cases, the *YAP1–MAML2* rearrangement and *GTF2I* mutation were both significant molecular events specific to MT and type A thymoma, respectively.

ARTICLE HISTORY

Received 18 June 2023

Revised 10 July 2023

Accepted 11 July 2023

KEYWORDS

Metaplastic thymoma; *YAP1–MAML2* rearrangement; *GTF2I* mutation; fluorescence *in situ* hybridization; next-generation sequencing

Introduction





Although thymoma is the most common primary mediastinal epithelial tumour, metaplastic thymoma (MT) is a rare and indolent type that accounts for <1% of all thymomas [1]. Despite its characteristic biphasic differentiation including solidly growing nests of epithelioid cells and bundles of spindle cells as background [2], MT lacks the classic histologic characteristics of thymomas, such as solid lobular growth, perivascular spaces and TdT-positive immature lymphocytes. MT is typically clinically asymptomatic [3], with a few rare exceptions having myasthenia gravis. It is most likely to be confused with type A thymoma with a bidirectional differentiation tendency and the A component of type AB thymoma. This confusion can make it more challenging to diagnose complicated cases. Recent studies in this area have demonstrated that type A thymoma frequently

harbours the *GTF2I* c.74146970T>A mutation [4], whereas MT frequently harbours the *YAP1–MAML2* gene rearrangement [5]. In this study, five cases of MT and four cases of type A thymoma with bidirectional differentiation trends were collected and analysed using immunohistochemistry, fluorescence *in situ* hybridization (FISH) and next-generation sequencing (NGS). The purpose of the study is to investigate the interpretation criteria and significance of molecular analysis in the diagnosis and differential diagnosis of MT.

Materials and methods

Patients and tumour specimens

Five cases of MT diagnosed in the Department of Pathology at the First Hospital of China Medical University from January 2021 to January 2023, were

CONTACT Minghao Wang  mhwang@cmu.edu.cn  Department of Neurosurgery, First Hospital of China Medical University, Shenyang, China; Liang Wang  lwang@cmu.edu.cn  Department of Pathology, First Hospital of China Medical University, Shenyang, China

© 2023 The Author(s). Published by Informa UK Limited, trading as Taylor & Francis Group

This is an Open Access article distributed under the terms of the Creative Commons Attribution-NonCommercial License (<http://creativecommons.org/licenses/by-nc/4.0/>), which permits unrestricted non-commercial use, distribution, and reproduction in any medium, provided the original work is properly cited. The terms on which this article has been published allow the posting of the Accepted Manuscript in a repository by the author(s) or with their consent.

included in this investigation. Three pathologists re-examined and verified all slides, including the immunohistochemistry analysis. In addition, four cases of type A thymomas that morphologically resembled MT were chosen for comparison due to their shared characteristics with MT, such as epithelial nests and spindle cells, ill-defined perivascular spaces, and little to no distribution of TdT-positive lymphocytes. All patients' clinical information was obtained from their medical records. The follow-up time was measured from the date of operation to that of the last telephone follow-up (Table 1). This study was approved by the Ethics Committee of the First Hospital of China Medical University. All patients agreed to the use of all relevant data and provided informed consent.

Immunohistochemistry

The formalin-fixed, paraffin-embedded (FFPE) tissues were cut to 4- μ m-thick sections. Immunohistochemical staining was carried out using an automated immunostainer (Roche Ventana Benchmark XT, Basel, Switzerland) following the manufacturer's instructions. A panel of ready-to-use immunohistochemical markers was used, which included Dako's primary antibodies: cytokeratin (CK, clone AE1/AE3), P63 (clone DAK-P63) and TdT (clone EP266), and Fuzhou Maixin's primary antibodies: CD3 (clone MX036), CD20 (clone L26, MX003), CD5 (clone MX052), CD117 (clone YR145), EMA (E29), vimentin (MX034), E-cadherin (MX020) and Ki-67 (clone MX 006). In addition, the primary antibody YAP1 (monoclonal antibody, 1:100, Santa Cruz Biotechnology Company, Santa Cruz, CA) was used for immunostaining. Positive expression of YAP1 was defined as nuclear positive signals in $\geq 10\%$ of cells.

FISH detection

A commercial FISH detection kit (Wuhan HealthCare Biotechnology, Wuhan, China) was used and operated according to the instructions to perform FISH tests on nine samples with three probes. Dual-colour FISH was performed with the *MAML2* break-apart probe, with the

green marker at the telomeric-proximal end and the orange marker at the centromeric-proximal end, and with the dual-colour *YAP1* break-apart probe, with the green marker at the telomeric-proximal end and the orange marker at the centromeric-proximal end. The dual-colour *YAP1-MAML2* fusion probe was used with orange fluorescein labelling the 5'-end of *YAP1* and green fluorescein labelling the 3'-end of *MAML2*. The results were observed under an automated fluorescence microscope (Zeiss AXIO, Imager Z2, Oberkochen, Germany). Since *YAP1* (11q22) and *MAML2* (11q21) are located only six mega-base pairs apart on the same chromosome, such a short distance may lead to misjudgement, no matter break-apart or fusion probes were adopted. Therefore, specific interpretation criteria need to be designed. We set the criteria for the break-apart probes as follows: rearrangement was considered when there is one signal point between the orange and green signals. For fusion probes, fusion was considered when the orange and green signals overlapped into yellow signals. A minimum of 200 cells were counted in each section, and the percentage of positive cells was calculated. Samples were determined to contain *MAML2* or *YAP1* rearrangements when the number of positive cells for break-apart probes was $\geq 50\%$ with break-apart probes; samples were determined to contain *YAP1-MAML2* fusions when the number of positive cells for fusion probes was $\geq 10\%$ with fusion probes.

DNA and RNA extraction

DNA and RNA were extracted from the nine FFPE samples using the automatic nucleic acid extractor EASY 12 (Amoy Diagnostics, Xiamen, China). The nucleic acids were then quantified using a Quantus or Qubit fluorometer. Then, according to the manufacturer's guidelines, the qualified DNA and RNA were used for library construction.

NGS detection

The probes targeting the *YAP1-MAML2* gene rearrangement and *GTF2I* gene mutation were designed

Table 1. Clinical information of nine cases of thymoma.

Case no.	Age	Sex	Myasthenia	Maximum diameter (cm)	Histotype	Masaoka-Koga staging	Treatment	Follow-up (months)
1	43	M	No	2.4	Metaplastic	I	Resection	Alive at 25
2	49	F	No	2.5	Metaplastic	I	Resection	Alive at 19
3	74	F	No	14 (cystic)	Metaplastic	I	Resection	Alive at 12
4	36	F	No	4.5	Metaplastic	I	Resection	Alive at 13
5	38	M	No	11	Metaplastic	I	Resection	Alive at 23
6	51	M	Yes	3	Type A	I	Resection	Alive at 17
7	55	F	No	5 (cystic)	Type A	I	Resection	Alive at 16
8	66	F	Yes	5.5	Type A	I	Resection	Alive at 8
9	69	M	No	7	Type A	I	Resection	Alive at 15

using ADx-HANDLE technology (Amoy Diagnostics, Xiamen, China), and they included extension and ligation arms, which were complementary to the target gene region. According to the status of the *YAP1*–*MAML2* gene arrangement, the following four fusion types were designed: *YAP1* exon1–*MAML2* exon2; *YAP1* exon2–*MAML2* exon2; *YAP1* exon5–*MAML2* exon2; and *YAP1* exon6–*MAML2* exon2. *YAP1* transcript: NM_001130145.3; *MAML2* transcript: NM_032427.4.

According to the mutation point coordinates of *GTF2I* gene ch7:74146970 T>A (p.L424H), two pairs of extension and ligation arms probes were designed, as follows: *GTF2I-L424H-1* (extension arm (5′-TCTTAATCACAAAACGAATCCTTCCTTTG-3′); ligation arm (5′-GGAAAA GAGGGTACGGGATCGTC-3′)) and *GTF2I-L424H-1* (extension arm (5′-TCTACTTACGGAATTCCTCGCTG-3′); ligation arm (5′-AGGTTCTATGTGATGAAGTTTGAGTT-3′)).

In addition, the detection of other gene mutations, such as *KRAS*, *TP53*, *NRAS*, *HRAS* and *PLOE*, was performed using the AmoyDx HANDLE Classic NGS Panel (Amoy Diagnostics, Xiamen, China) [6]. After the libraries were prepared, Illumina NextSeq 500 (paired-end reads, 2 × 150 cycles) was used for RNA (fusions) and DNA sequencing (SNVs, InDels, CNVs), and the data were then qualified and analysed using an AmoyDx ANDAS Data Analyzer (Amoy Diagnostics, Xiamen, China).

Results

Histology and immunohistochemistry

The MTs all had a solid growth pattern (except for one case with cystic formation), lacked lobular architecture and perivascular spaces, and displayed a mixture of epithelial cell nests and their surrounding spindle cell bundles, indicating bidirectional differentiation, with only a few scattered lymphocytes. Epithelial cells expressed CK, P63 and E-cadherin, whereas spindle cells expressed vimentin and EMA. CD20 was not expressed by either cell type. A small number of CD3- and CD5-positive lymphocytes were found primarily in the spindle cell area, but CD1a and TdT were negative. Nuclear positive expression of *YAP1* was found in three of the five cases of MT, with the positive expression primarily found in spindle cells (Figure 1). Perivascular spaces (3/4), microcystic and glandular structures were occasionally seen in four cases of the type A thymoma, in addition to different proportions of epithelial cells and spindle cell components. Except for the lymphocytes, cells in type A thymomas expressed CK, p63 and CD20 but were negative for vimentin (Figure 1). There was only one case with a nuclear positive expression of *YAP1*.

FISH analysis

The number of cells positively separated signals was >50% in all the five MT cases, no matter detected by the *YAP1* dual-colour break-apart probe or the *MAML2* dual-colour break-apart probe, whereas the percentage of *YAP1*- or *MAML2*-positive cells was no more than 40% in all four cases of the type A thymoma. The detection of the *YAP1*–*MAML2* fusion probe revealed that the number of fusion cells exceeded 10% in all five of the MT cases, but not in any type A thymoma (Figure 2).

NGS sequencing

The *YAP1*–*MAML2* gene rearrangement was detected in all MTs (cases 1–5), and dual fusions were found in cases 1, 2 and 5 (Table 2). The *GTF2I* p.L424H point mutation was detected in all four cases of type A thymoma. The NGS detection results were highly consistent with the immunohistochemistry and FISH results. Furthermore, the mutations of *KRAS* and *TP53* were not detected. However, the *POLE* p.R712C and *HRAS* p.K117N mutations were detected in two cases of MT (cases 1 and 3), and the *HRAS* p.I24N and *NRAS* p.Q61K mutations were detected in two cases of the type A thymoma (cases 7 and 8).

Discussion

Clinically, MT does not usually exhibit signs of myasthenia gravis, not like other types of thymoma may lead to blood vessel damage, postoperative myasthenic crisis, pain, and a higher risk of infections [7]. To date, only two cases of myasthenia have been documented with MT [8], and these may be related to the relatively high number of T lymphocytes that are TdT-positive in the tissue [9]. MT is reported to usually have a solid growth pattern, with cystic formation in only one of nine cases [10]. It is distinguished histologically by nests of varying sizes of epithelial cells surrounded by bundles of spindle cells, indicating bidirectional differentiation. MT lacks fibrous septa, perivascular spaces and TdT-positive T lymphocytes. These morphological changes are frequently confused with type A or the A component in type AB thymoma. At this time, immunohistochemistry is frequently required for identification, and in challenging cases, molecular testing is even necessary to reach a final diagnosis.

Epithelial cells in MT expressed CK, P63 and E-cadherin, whereas spindle cells expressed vimentin

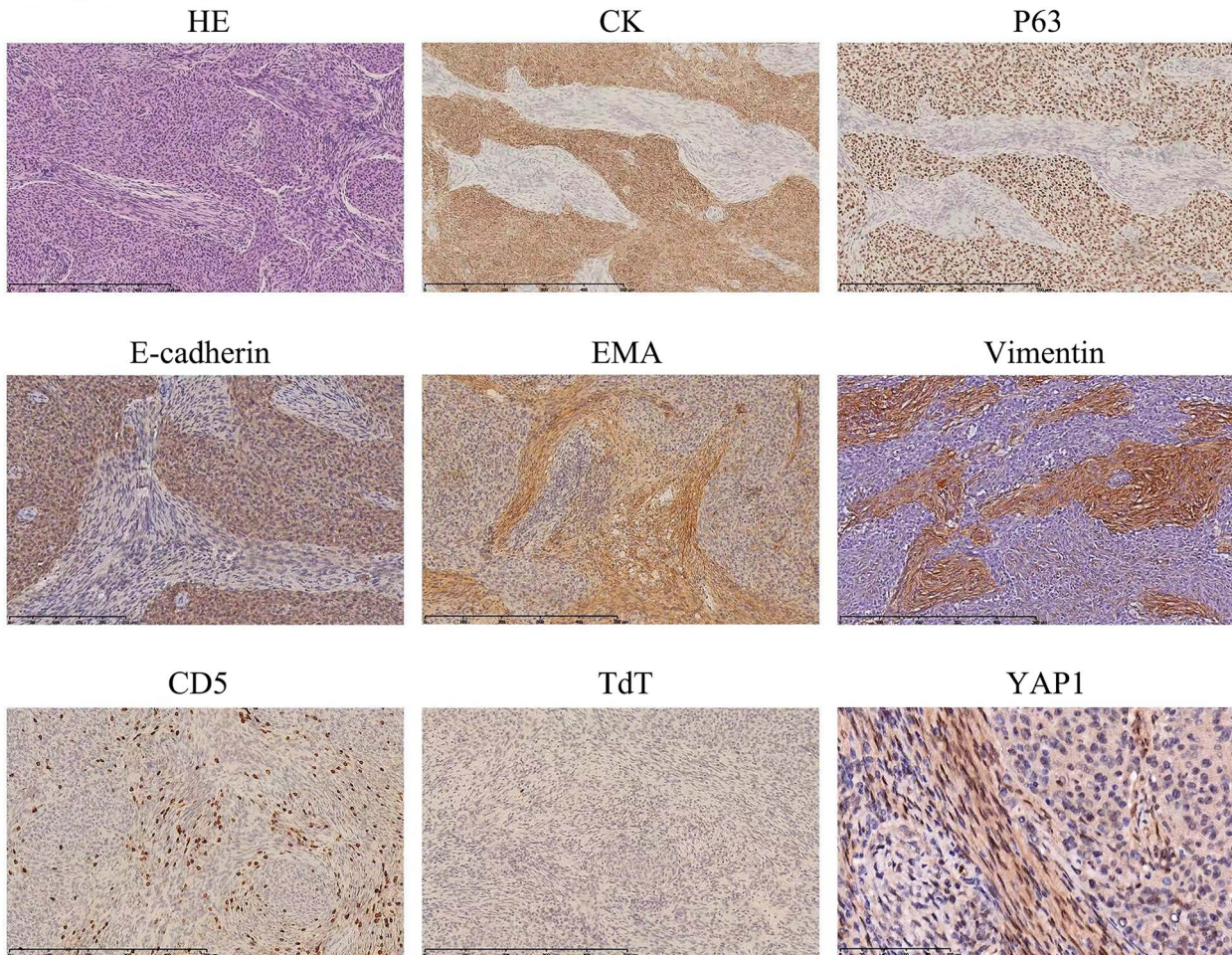
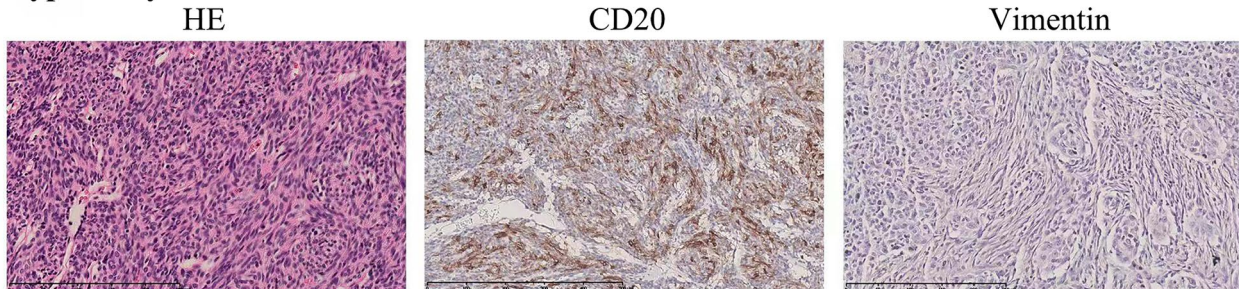
Metaplastic thymoma**Type A thymoma**

Figure 1. The histological characteristics and immune profiles of metaplastic thymoma and type a thymoma. In the metaplastic thymoma, the admixture of epithelial cell nests was surrounded by spindle cell bundles. Epithelial cells express CK, P63 and E-cadherin, whereas spindle cells express EMA and vimentin. A small number of CD5-positive cells were predominantly found in the spindle cell area, but their TdT was negative and they had nuclear YAP1 expression. In the type a thymoma, a small number of short, spindle-shaped cells are seen among the epithelial nests, expressing CD20 but negative for vimentin.

and EMA. A small number of CD3- and CD5-positive lymphocytes were found primarily in the spindle cell area, but they were negative for CD1a and TdT. Type A thymoma cells expressed CD20 as well as CK and P63 but lacked vimentin expression. Although immunohistochemistry aids in the diagnosis of MT, there are still some challenges in diagnosing difficult cases.

Some studies have found that it does have the *YAP1-MAML2* gene rearrangement, while MT does not have the *GTF2I* c.74146970T>A point mutation, which can be found in type A thymoma [11]. Our NGS detection of four cases of type A thymoma confirmed that they all had the *GTF2I* c.74146970T>A point mutation, while the five MT cases were all negative. In contrast,

the *YAP1*–*MAML2* gene rearrangement was found in all five MT cases, according to the NGS sequencing results. This further demonstrates the importance of detecting

the *GTF2I* c.74146970T>A point mutation and *YAP1*–*MAML2* gene rearrangement in a differential diagnosis and the diagnosis of challenging cases.

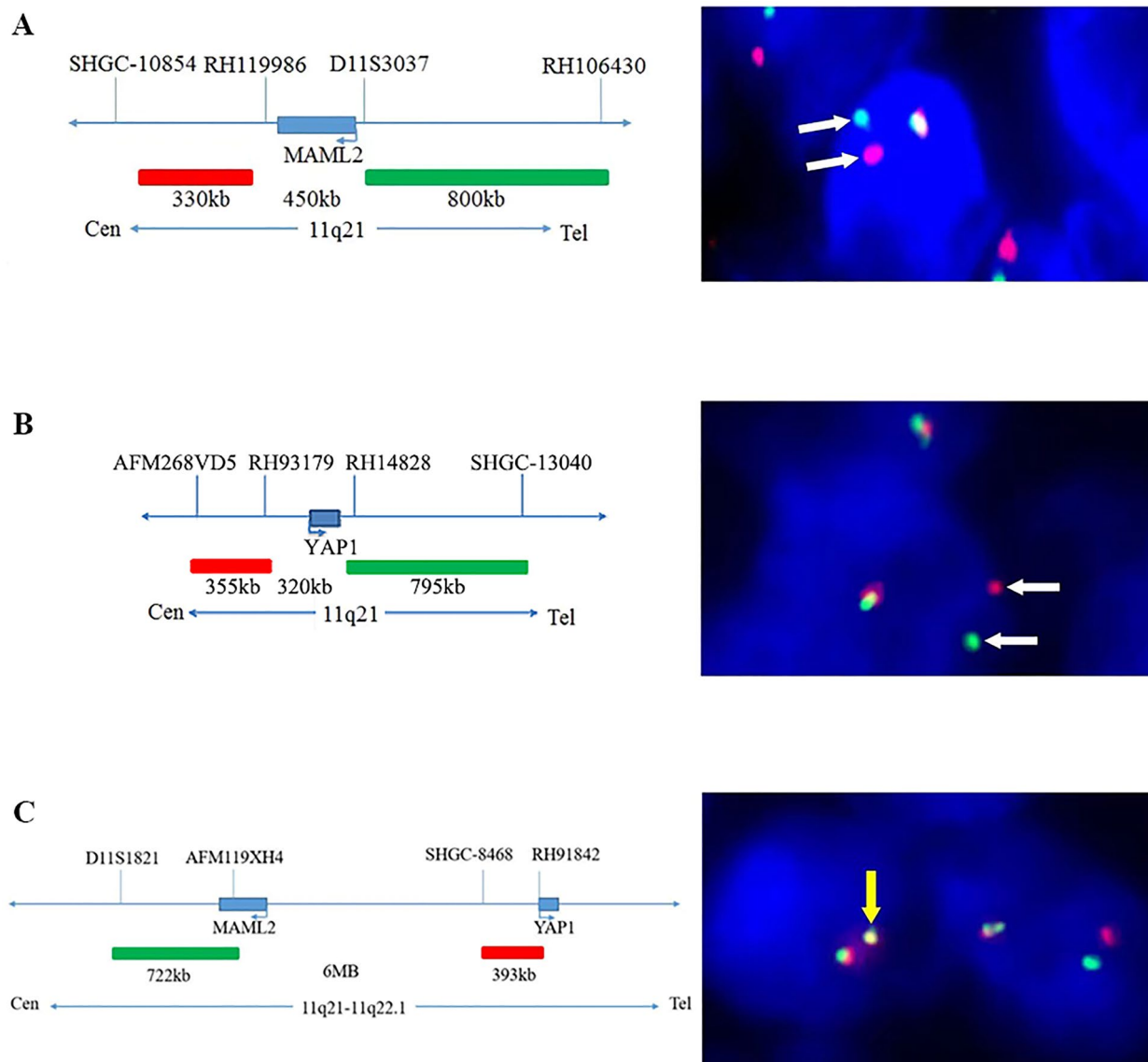


Figure 2. The characteristics of probes and representative results of the FISH analysis. The labelling of the dual-colour break-apart probes *MAML2* (A) and *YAP1* (B) and the fusion probe *YAP1*–*MAML2* (C), respectively, with corresponding representative positive cells in FISH analysis. The white arrows represent separate signals, while the yellow arrows represent fusion signals.

Table 2. NGS results of all nine cases of thymoma.

Case no.	Fusion	Copies	GTF2I Mut/Freq	Other Mut/Freq
1	YAP1:NM_001130145.3:exon5-MAML2:NM_032427.4:exon2	8351	None	POLE/48.31%
	YAP1:NM_001130145.3:exon6-MAML2:NM_032427.4:exon2	2221		
2	YAP1:NM_001130145.3:exon5-MAML2:NM_032427.4:exon2	13,137	None	
	YAP1:NM_001130145.3:exon6-MAML2:NM_032427.4:exon2	5538		
3	YAP1:NM_001130145.3:exon1-MAML2:NM_032427.4:exon2	10,017	None	HRAS/48.09%
4	YAP1:NM_001130145.3:exon1-MAML2:NM_032427.4:exon2	13,244	None	
5	YAP1:NM_001130145.3:exon5-MAML2:NM_032427.4:exon2	8209	None	
	YAP1:NM_001130145.3:exon6-MAML2:NM_032427.4:exon2	3193		
6	None		Yes/38.07%	
7	None		Yes/38.43%	HRAS/46.11%
8	None		Yes/37.11%	NRAS/40.21%
9	None		Yes/36.48%	

Detecting *MAML2-CRTC1* rearrangement in mucoepithelioid carcinoma using *MAML2* break-apart probes is distinct from detecting *YAP1-MAML2* rearrangement in MT. With *MAML2* located at 11q21 and *CRTC1* at 19p13, the two genes are on different chromosomes. In contrast, *YAP1* and *MAML2* are located on the same chromosome, spaced only six mega-base pairs apart. When *MAML2* or *YAP1* breaks in MT, the orange and green break-apart signals usually show a relatively narrow separation space [12].

If we adhere to the previous criteria, i.e. the distance between the orange and green signals being thrice the size of the signal, with the proportion of positive cells being $\geq 20\%$ (using FISH to identify the *MAML2-CRTC1* rearrangement) [3], all five MT cases would be negative. If we set the criteria as the distance between the orange and green break-apart signals being ≥ 1 , with the proportion of positive cells being $\geq 20\%$, half of type A thymomas in the current study would be positive. Therefore, the interpretation criteria for determining whether or not rearrangements exist in *YAP1-MAML2* using FISH with *YAP1* or *MAML2* break-apart probes or *YAP1-MAML2* fusion probes remain to be discussed. However, when we set the separation criteria for the orange and green signals to ≥ 1 signal distances, with the criteria for positive cells with break-apart and *YAP1-MAML2* fusion probes to $\geq 50\%$ and 10% , respectively, the test results were highly consistent with the NGS results. However, our case numbers were limited, and the tentative criteria used here would only serve as a reference. More cases should be tested to verify the correct interpretation criteria.

As the spindle cell component of MT expresses vimentin while the epithelial cell component expresses E-cadherin and the two cellular components are gradually merged, it has been proposed that this is an epithelial-mesenchymal transition (EMT) phenomenon [1]. Picco et al. discovered that the *YAP1-MAML2* gene rearrangement could increase YAP1 signalling *in vitro* [13]. The nuclear-localized expression of YAP1 in thymomas with the *YAP1-MAML2* gene rearrangement has been confirmed by Sekine et al. [12] The Hippo pathway, which is closely related to EMT, is transcriptionally activated as evidenced by the nuclear-localized expression of YAP1 [14,15]. In three out of the five MT cases, immunohistochemistry revealed nuclear localized expression of YAP1, but this expression was not diffuse and was primarily nuclear positivity in spindle cells. One case of positive YAP1 expression was also identified in a type A thymoma. It is thus clear that further research is required to understand the expression and significance of YAP1 in MT.

Conclusions

For the diagnosis and differential diagnosis of challenging cases, the *YAP1-MAML2* rearrangement and *GTF2I* mutation were both significant molecular events specific to MT and type A thymoma, respectively. Research into the molecular events in MT and associated molecular functional studies would not only help with difficult diagnostic cases but also elucidate novel information that could aid in the development of precisely targeted treatments.

Author contributions

Minghao Wang: manuscript writing, data acquisition and funding acquisition. Hongtao Xu: conducting the experiments, data acquisition and interpretation of the data. Qiang Han: data acquisition and interpretation of the data. Liang Wang: manuscript writing, English editing, project administration and funding acquisition. All authors agree to be accountable for all aspects of the work.

Ethical approval

Ethical approval for this study was obtained from the institutional ethics review boards of the First Affiliated Hospital of China Medical University.

Consent form

Informed consent was obtained from the patient's guardian for the publication of this case and any accompanying images. The copies of the written consents are available for review by the Editor-in-Chief of this journal. Writing consent to participate was provided by the patient's guardian for the present research.

Disclosure statement

The authors declare that they have no competing interests.

Funding

This study was supported by grants from the Natural Science Foundation of Liaoning (2021-MS-160, 2022-MS-218).

Data availability statement

The datasets supporting the conclusions of this article are included within the article.

References

- [1] Liu B, Rao Q, Zhu Y, et al. Metaplastic thymoma of the mediastinum. A clinicopathologic, immunohistochemical, and genetic analysis. *Am J Clin Pathol.* 2012;137(2): 1–8. doi: [10.1309/AJCP0T1JFYLMPHMI](https://doi.org/10.1309/AJCP0T1JFYLMPHMI).

- [2] Travis WB, Burke AP, Marx A, et al. WHO classification of tumors of the lung, pleura, thymus and heart. 4th ed. Lyon: IRAC; 2015.
- [3] Zhao J, Zhao R, Xiang C, et al. YAP1–MAML2 fusion as a diagnostic biomarker for metastatic thymoma. *Front Oncol.* 2021;11:692283. doi: [10.3389/fonc.2021.692283](https://doi.org/10.3389/fonc.2021.692283).
- [4] Wells K, Lamrca A, Papaxoinis G, et al. Unique correlation between GTF2I mutation and spindle cell morphology in thymomas (type A and AB thymomas). *J Clin Pathol.* 2023;76(7):463–466. doi: [10.1136/jclinpath-2021-207837](https://doi.org/10.1136/jclinpath-2021-207837).
- [5] Vivero M, Davineni P, Nardi V, et al. Metaplastic thymoma: a distinctive thymic neoplasm characterized by YAP1–MAML2 gene fusions. *Mod Pathol.* 2020;33(4):560–565. doi: [10.1038/s41379-019-0382-x](https://doi.org/10.1038/s41379-019-0382-x).
- [6] Liu Y, Wu S, Zhou L, et al. Pitfalls in RET fusion detection using break-apart FISH probes in papillary thyroid carcinoma. *J Clin Endocrinol Metab.* 2021;106(4):1129–1138.
- [7] Georgiev A, Hilendarov A, Tsvetkova S, et al. Thymoma type B2 progression, due to fear of contamination, in association with hydrocephalus: a case report of avoidant behavior during COVID-19 pandemic. *Radiol Case Rep.* 2022;17(3):680–684. doi: [10.1016/j.radcr.2021.12.028](https://doi.org/10.1016/j.radcr.2021.12.028).
- [8] Kang G, Yoon N, Han J, et al. Metaplastic thymoma: report of 4 cases. *Korean J Pathol.* 2012;46(1):92–95. doi: [10.4132/KoreanJPathol.2012.46.1.92](https://doi.org/10.4132/KoreanJPathol.2012.46.1.92).
- [9] Tajima S, Yanagiya M, Sato M, et al. Metaplastic thymoma with myasthenia gravis presumably caused by an accumulation of intratumoral immature T cells: a case report. *Int J Clin Exp Pathol.* 2015;8(11):15375–15380.
- [10] Poorabdollah M, Mehdizadeh E, Mohammadi F, et al. Metaplastic thymoma: report of an unusual thymic epithelial neoplasm arising in the wall of a thymic cyst. *Int J Surg Pathol.* 2009;17(1):51–54. doi: [10.1177/1066896908315754](https://doi.org/10.1177/1066896908315754).
- [11] Marx A, Belharazem D, Lee DH, et al. Molecular pathology of thymomas: implications for diagnosis and therapy. *Virchows Arch.* 2021;478(1):101–110. doi: [10.1007/s00428-021-03068-8](https://doi.org/10.1007/s00428-021-03068-8).
- [12] Sekine S, Kiyono T, Ryo E, et al. Recurrent YAP1–MAML2 and YAP1–NUTM1 fusions in poroma and porocarcinoma. *J Clin Invest.* 2019;129(9):3827–3832. doi: [10.1172/JCI126185](https://doi.org/10.1172/JCI126185).
- [13] Picco G, Chen ED, Alonso LG, et al. Functional linkage of gene fusions to cancer cell fitness assessed by pharmacological and CRISPR–Cas9 screening. *Nat Commun.* 2019;10(1):2198. doi: [10.1038/s41467-019-09940-1](https://doi.org/10.1038/s41467-019-09940-1).
- [14] Guo Q, Quan MY, Xu L, et al. Enhanced nuclear localization of YAP1-2 contributes to EGF-induced EMT in NSCLC. *J Cell Mol Med.* 2022;26(4):1013–1023. doi: [10.1111/jcmm.17150](https://doi.org/10.1111/jcmm.17150).
- [15] Shao DD, Xue W, Krall EB, et al. KRAS and YAP1 converge to regulate EMT and tumor survival. *Cell.* 2014;158(1):171–184. doi: [10.1016/j.cell.2014.06.004](https://doi.org/10.1016/j.cell.2014.06.004).